

Virtual biopsy of rat tympanic membrane using higher harmonic generation microscopy

Wen-Jeng Lee

National Taiwan University
Department of Electrical Engineering
Taipei, 10617, Taiwan
and
National Taiwan University Hospital
Department of Medical Imaging
Taipei, 10051, Taiwan

Chia-Fone Lee

Tzu Chi General Hospital
Department of Otolaryngology
Hualien, 97004, Taiwan
and
Tzu Chi University
Department of Medicine
Hualien, 97004, Taiwan

Szu-Yu Chen

National Taiwan University
Department of Electrical Engineering
Taipei, 10617, Taiwan
and
National Taiwan University
Graduate Institute of Photonics and Optoelectronics
Taipei, 10617, Taiwan

Yuh-Shyang Chen

Tai-Tung Christian Hospital
Department of Otolaryngology
Tai-Tung, 95048, Taiwan

Chi-Kuang Sun

National Taiwan University
Department of Electrical Engineering
Taipei, 10617, Taiwan
and
National Taiwan University
Graduate Institute of Photonics and Optoelectronics
Taipei, 10617, Taiwan
and
Academia Sinica
Research Center for Applied Sciences
Taipei 11529, Taiwan

1 Introduction

Tympanic membrane (TM) is the first component in the middle ear mechanical conduction system for sound transmission. It is a very thin membrane composed of three layers: external stratified epithelium, middle fibrous connective tissue, and internal epithelium. The external stratified epithelium

Abstract. Multiharmonic optical microscopy has been widely applied in biomedical research due to its unique capability to perform noninvasive studies of biomaterials. In this study, virtual biopsy based on back-propagating multiple optical harmonics, combining second and third harmonics, is applied in unfixed rat tympanic membrane. We show that third harmonic generation can provide morphologic information on the epithelial layers of rat tympanic membrane as well as radial collagen fibers in middle fibrous layers, and that second harmonic generation can provide information on both radial and circular collagen fibers in middle fibrous layers. Through third harmonic generation, the capillary and red blood cells in the middle fibrous layer are also noted. Additionally, the 3-D relationship to adjacent bony structures and spatial variations in thickness and curvature are obtained. Our study demonstrates the feasibility of using a noninvasive optical imaging system for comprehensive evaluation of the tympanic membrane. © 2010 Society of Photo-Optical Instrumentation Engineers. [DOI: 10.1117/1.3469848]

Keywords: tympanic membrane; middle ear modeling; multiharmonic generation microscopy.

Paper 09363RR received Aug. 19, 2009; revised manuscript received May 29, 2010; accepted for publication Jun. 2, 2010; published online Aug. 2, 2010.

is composed of several layers of cells. The middle fibrous layer is composed of fibroblasts, collagen fibrils, blood vessels, and lymphatics. The internal epithelium is composed of a single layer of cells. The collagen framework is arranged into external radial and internal nonradial layers.¹⁻³ Sound from the air vibrates the TM, which leads to motion of the auditory ossicles in the middle ear cavity. Animal and mathematical models have been used for research of sound conduction in the past. To understand the mechanisms of the middle ear in mathematical models, the relevant system parameters (thick-

Address all correspondence to: Chi-Kuang Sun, National Taiwan University, Graduate Institute of Photonics and Optoelectronics, R319, 2nd EE building, 1 Roosevelt Rd. Sec. 4, Taipei, 10617, Taiwan. Tel: 886-2-33665085; Fax: 886-2-33663614. E-mail: sun@cc.ee.ntu.edu.tw and Yuh-Shyang Chen, Tai-Tung Christian Hospital, Department of Otolaryngology, Tai-Tung, 95048, Taiwan. E-mail: yschen@ntu.edu.tw

ness and shape of the TM, damping, elasticity and geometry of the ossicles, etc.) are necessary. 3D spatial information of the TM is essential for further functional studies of the middle ear.^{4,5}

In clinical disease diagnosis, biopsy is traditionally recognized as the gold standard. However, biopsy requires the removal, fixation, and staining of the tissues or cells. Such histological procedures are not only time consuming but also invasive and painful. Additionally, the histological preparation might cause a decrease in the thickness of the central region of the TM from 16 to 35%, depending on the position within the TM.⁶ Most importantly, biopsy of the TM can risk hearing loss. Therefore, a noninvasive *in-vitro* or *in-vivo* optical virtual biopsy, which can provide highly penetrative 3-D images with a submicron spatial resolution, and also provide information about the change of TM resulting from disease processes, is desired.

Higher harmonic generation microscopy (HGM) can provide a noninvasive biopsy tool with excellent 3-D spatial resolution because of its virtual transition and nonlinear characteristics.^{7,8} Harmonic generation itself is known to deposit no energy in the matter with which it interacts because of the energy-conservation characteristics of the generation. The generated second harmonic generation (SHG) and third harmonic generation (THG) intensities depend on the square and cube of the incident light intensity, respectively. Similar to the multiphoton-induced fluorescence process, this nonlinear dependence allows localized excitation and is ideal for intrinsic optical sectioning in scanning laser microscopy. SHG and THG signals can be acquired simultaneously with backward collection geometry (epidetection mode) without the need of exogenous contrast agents.^{9,10} Thus, it is suitable for *in-vivo* observation.^{11,12} The purpose of this study is to demonstrate the feasibility of using nonlinear optical imaging as a means of virtual biopsy. Backward-collected (epi)-SHG and THG were used to image excised rat TM.

2 Methods

One healthy rat (Wistar) weighing about 35 g was used. The rat was euthanized by an overdose of anesthetic (phenobarbital) injected into the peritoneum, and immediately decapitated. The ear was determined to be free from middle ear infections and was pristine and transparent. The right TM was used and prepared similar to the method described in recent studies.^{6,13} However, we did not dissect the TM out of its surrounding bone. The whole middle ear with intact tympanic membrane and surrounding bone was observed in this study. Thus, the intact membrane was observed under conditions that are close to a natural situation. The whole excised middle ear with intact tympanic membrane was rinsed in phosphate buffered solution for hydration during imaging. The experiment procedure was reviewed and approved by the Institutional Animal Care and Use Committee in National Taiwan University Hospital.

The study of the harmonic generation microscopy of fresh intact rat tympanic membrane was performed using a home-built femtosecond Cr:forsterite laser centered at 1230 nm with a 130-fs pulse width and a 110-MHz repetition rate.^{10,14} The spectral full width half maximum of the laser output was 15 nm. The infrared laser beam was first shaped by a tele-

scope and then directed into a modified beam scanning system (Olympus Fluoview300) and an upright microscope (Olympus BX-51). An infrared (IR) water-immersion objective (Olympus LUMplanFL/IR 60×/NA 0.9/working distance 2 mm) was used to focus the laser beam into the observed specimen.

The observed specimen was mounted on the microscope stage. The generated epi-SHG and epi-THG signals were collected using the same objective used to focus the laser beam. A chromatic beamsplitter [Chroma Technology (Rockingham, Vermont) 865dcxru] was used to direct the backward SHG and THG signals into a home-built photon detection system. In this photon detection system, the backward SHG and THG were separated by another chromatic beam splitter (Chroma Technology 490DRXR) and detected by two separate photomultiplier tubes (PMTs) (Hamamatsu R4220P for THG and Hamamatsu R943-02 for SHG) with 410-nm (THG) and 615-nm (SHG) narrow-band interference filters (Chroma Technology D410/10× and D615/10×). An average illumination power of 90 mW was applied to the sample surface during the study. The excised rat middle ear was placed on the microscope stage with the external surface of the eardrum facing upward to the objective lens to mimic the *in-vivo* condition. The adopted scanning rate of Fluoview300 was 1000 lines/s, or about four frames per second for one 256 × 256 resolution image with a 240 × 240- μm field of view. By moving the axial position of the stage, about 200 frames were acquired to obtain a 240 × 240 × 200- μm 3-D imaging slab covering the whole depth of the tympanic membrane. Since the spatial step size (around 1 μm) was much greater than the THG lateral resolution (around 0.4 μm ^{12,15}), higher spatial resolution could be easily achieved in the future with a finer step size during the scan. Low resolution was applied just to mimic the future clinical situation for much reduced acquisition time. Scanning was repeated after lateral translation of the motorized microscope stage. The 3-D image of the whole tympanic membrane can be obtained by combining all imaging blocks.

3 Results

Figure 1 is a photograph of the rat TM used in this study. The TM was not excised from the surrounding bone. The TM can be divided into two parts (pars flaccida and pars tensa). Figure 2 shows the obtained virtual biopsy image of pars tensa from SHG and THG microscopy. THG reveals the spatial structure of the external epithelial layer¹⁶ as well as the radial collagen fibers in the middle fibrous layer. Both the radial and circular collagen fibers in the middle fibrous layer were revealed by epi-SHG.¹⁷ Figure 3, from the peripheral portion of pars tensa, shows red blood cells in the capillaries of the middle fibrous layer. The imaging features of red blood cells, capillaries, and epithelial cells are similar to those found in oral mucosa and skin from our previous studies of harmonic generation microscopy.¹⁰⁻¹²

Figure 4 shows an axial image of pars tensa using the multiharmonic generation microscope. The cross section of the TM is displayed as the white, curved band. In Fig. 4, the upper surface is the external surface and the lower surface is the medial surface. The thickness of the membrane was measured by using the full width at half maximum (FWHM) of the intensity profile taken perpendicularly through the cross

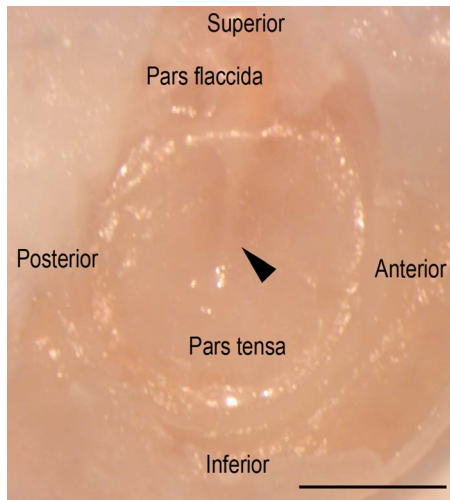


Fig. 1 A photograph of the rat TM used in this study. The TM was not excised from the surrounding bone. The manubrium of the malleus (arrow) can be seen on the central part of the TM. The two parts of the TM (pars flaccida and pars tensa) were labeled. Scale bar: 1 mm.

section from the upper surface toward the lower surface. The TM is very thin for the large part, only about $13.5 \mu\text{m}$. The pars flaccida is thicker than the pars tensa. The membrane is thickest around the peripheral region, becomes gradually thinner when moving inward, remains at an almost constant small value in the middle zone, and finally thickens again toward the manubrium of the malleus.

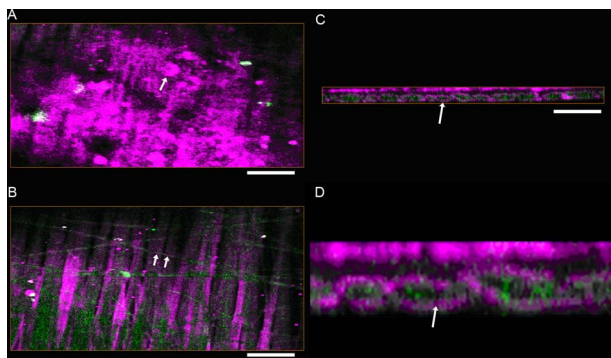


Fig. 2 3-D harmonic generation microscopy “virtual biopsy” images obtained from pars tensa of the tympanic membrane. THG is shown by pink and SHG is shown by green. THG is sensitive to the region of inhomogeneity, and thus it can provide the interface information and reveal the structure of outer epithelial layers as well as the middle radial collagen fibers. SHG arises from noncentrosymmetry and highly organized nanostructures; middle collagen fibers in tympanic membrane provide strong SHG contrast. (a) Horizontal section of external stratified epithelium shows cells (arrow) in the epithelium. (b) Horizontal section of middle fibrous connective tissue layer shows radial and circular fibers (arrows). There are SHG signals from both radial and circular fibers. The radial fibers in the middle fibrous layer also have a strong THG signal. (c) Cross sectional reconstructed image of whole thickness of tympanic membrane, and (d) magnified image of central portion of (c) shows strong THG signals from external stratified epithelium. The radial fibers (pink color) in the middle fibrous layer are interconnected and arranged in a chain shape (arrow). Scale bar: $50 \mu\text{m}$. (Color online only.)

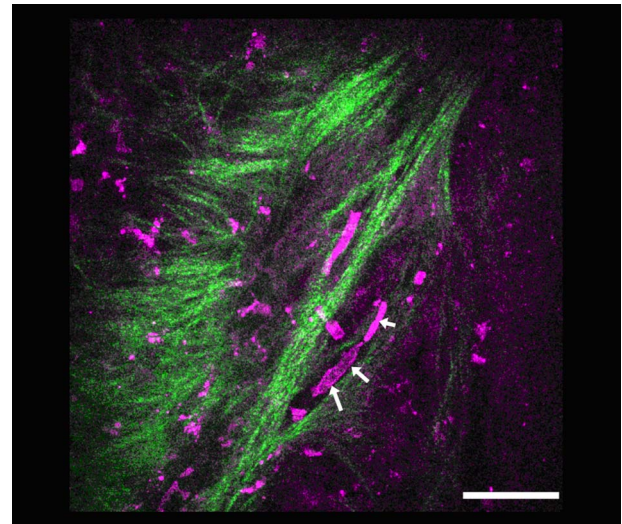


Fig. 3 Horizontal section of one portion of middle fibrous connective tissue layer. THG revealed red blood cells (arrows) in capillaries. Scale bar: $50 \mu\text{m}$. (Color online only.)

Figure 5 reveals the potential to image a large area of TM. By computer reconstruction of consecutive imaging blocks, a reconstructed 3-D image of the whole TM can be obtained. The 3-D relationship to the adjacent bony structure, spatial variation in curvature, and thickness can all be studied by this method. The plot shows a gradual increase in the thickness in the central region from the inferior to the superior region, and the thickness of TM was small relative to the diameter perpendicular to the manubrium of the malleus. The TM is thinnest in the central inferior region. The normal conical shape of the TM can also be clearly visualized.

4 Discussion

In this study, we confirmed that this method is capable of accurately resolving the minimum thickness of $10 \mu\text{m}$ in the rat eardrum with a high axial resolution around $1 \mu\text{m}$. A remarkable finding in this study is that the rat TM is very thin for the large part, only about $13.5 \mu\text{m}$. We also found that the pars flaccida is thicker than the pars tensa. Membrane thickness varies with position: the membrane is thicker from the center to the peripheral edge and close to a recent study of rat TM thickness of $14.88 \pm 1.85 \mu\text{m}$.¹⁸ In addition, the thickness map constructed in this study shows that the membrane is thickest around the peripheral region, becomes gradually thinner when moving inward, remains at an almost constant small value in the middle zone, and finally thickens again toward the manubrium of the malleus.

The thickness distribution of TM has been studied by Kuypers et al. in fresh conditions by the use of the optical sectioning capability of a confocal microscope.^{6,13} However, a special dye (Van Gieson dye) was required to stain the collagen in the tympanic membrane, and the membrane had to be flattened and dissected from its surrounding bone, as the lens used had a working distance limited to $230 \mu\text{m}$. This method is not suitable for *in-vivo* study, and the histological three-layered structure of the eardrum as well as the global 3-D shape of the membrane cannot be resolved.

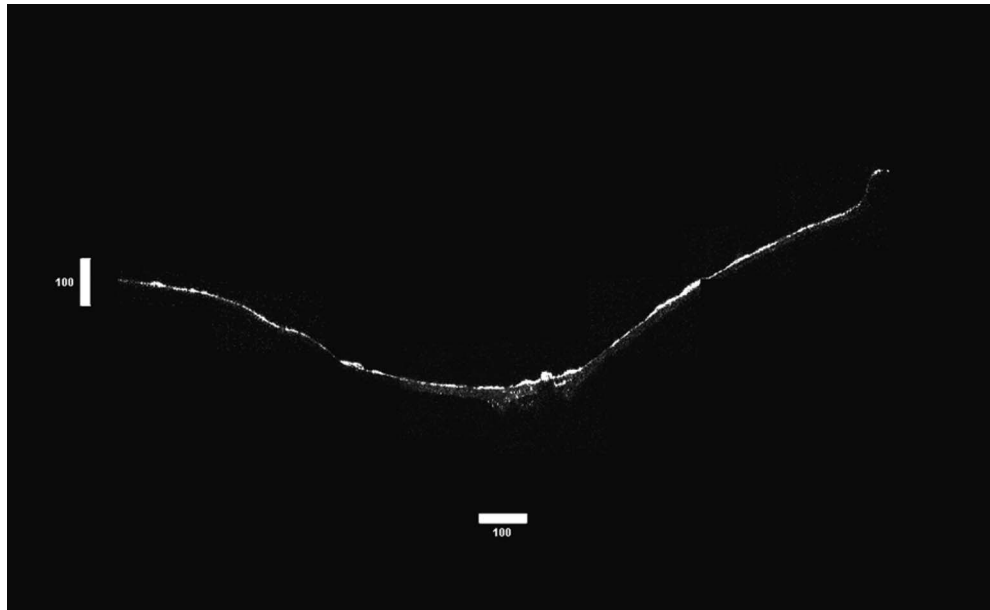


Fig. 4 A complete scan of the cross section of a right rat TM. The scan was obtained by aligning 200 axial images, each $240 \times 240 \mu\text{m}$ wide. Scale bar: $100 \mu\text{m}$.

Acute otitis media (AOM) is a very common childhood disease. Collagen organization of the TM is modified during the inflammatory stage and the healing process.¹⁹ Radial collagen fibers in the TM play an important role in the conduction of sound above 4 kHz.²⁰ Collagen orientation of human cadaver tympanic membranes has been studied meticulously by Jackson et al. using multiphoton microscopy.²¹ However, the membrane also had to be flattened and dissected from its surrounding bone, as the depth of field of its multiphoton microscopy is $0.9 \mu\text{m}$. Our study confirms that our method

could provide information on the collagen framework in the middle fibrous layer of TM without the use of fluorescence and exogenous markers.

In-vivo evaluation of the TM structure and pathology will be possible in the future using harmonic generation imaging by integrating an endoscope system. Besides the role of non-invasive diagnosis of TM disease, high harmonic generation microscopy may aid the surgeon to perform myringotomy. Myringotomy is a common surgical procedure for treating middle ear infection. In this procedure, a small incision is made on the TM to drain pus from the middle ear cavity. We propose that harmonic generation microscopy can guide the myringotomy procedure by identifying the orientation of the supporting radial collagen fibrils. The surgical section should be parallel to the radial collagen fibrils. In this way, the damage to the TM during surgery can be minimized. Our study demonstrates the feasibility of using a noninvasive optical imaging system¹² for comprehensive evaluation and possible surgical guidance of the TM.

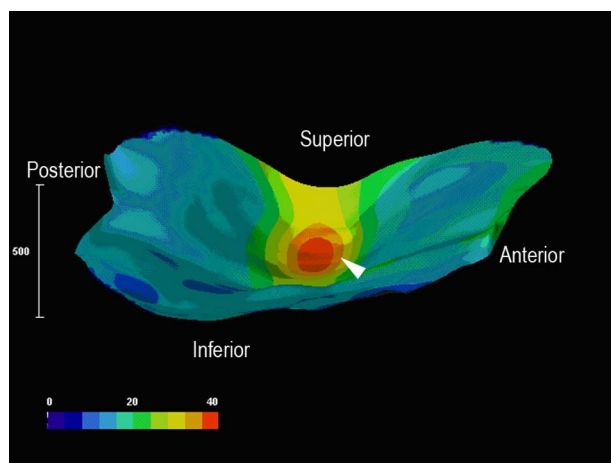


Fig. 5 3-D reconstructed image of the whole tympanic membrane. The thickness profile of the tympanic membrane was presented using a color map and the unit in this map is in micrometers. The central portion of the membrane is depressed because it attached to the underlying manubrium of the malleus, a small ossicle in the middle ear cavity. The normal conical shape of the intact tympanic membrane can be clearly visualized by this image. The size of the scale bar is $500 \mu\text{m}$. (Color online only.)

5 Conclusion

In summary, harmonic generation microscopy can noninvasively evaluate the anatomy of TM in distinguishing external epithelium and middle fibrous layers of intact tympanic membrane clearly. The spatial arrangement of radial and circular collagen fibrils can be observed. The capillary and red blood cells in the middle fibrous layer are noted. The 3-D relationship to adjacent bony structures and spatial variations in thickness and curvature can also be obtained. Epi-mode harmonic generation microscopy may enable *in-vivo* virtual biopsy to aid in the pathological evaluation of the TM.

Acknowledgments

This work was supported by grants from the National Health Research Institute of Taiwan through NHRI-EX98-9201EI,

NTU Center for Medical Excellence, NTU grant 98R0334, the Buddhist Tzu Chi General Hospital (TCRD 9703 and 9704), and the National Science Council (NSC 97-2314-B-002-150-MY2) of Taiwan.

References

1. F. R. Johnson, R. M. McMinn, and G. N. Atfield, "Ultrastructural and biochemical observations on the tympanic membrane," *J. Anat.* **103**(pt 2), 297–310 (1968).
2. D. J. Lim, "Structure and function of the tympanic membrane: a review," *Acta Otorhinolaryngol. Belg.* **49**(2), 101–115 (1995).
3. K. Magnuson, S. Hellström, and B. Magnuson, "Structural changes in the rat tympanic membrane following repeated pressure loads," *Eur. Arch. Otorhinolaryngol.* **252**(2), 76–82 (1995).
4. M. Gaihede, D. Liao, and H. Gregersen, "In vivo areal modulus of elasticity estimation of the human tympanic membrane system: modelling of middle ear mechanical function in normal young and aged ears," *Phys. Med. Biol.* **52**(3), 803–814 (2007).
5. C. F. Lee, P. R. Chen, W. J. Lee, J. H. Chen, and T. C. Liu, "Three-dimensional reconstruction and modeling of middle ear biomechanics by high-resolution computed tomography and finite element analysis," *Laryngoscope* **116**(5), 711–716 (2006).
6. L. C. Kuypers, J. J. Dirckx, W. F. Decraemer, and J. P. Timmermans, "Thickness of the gerbil tympanic membrane measured with confocal microscopy," *Hear. Res.* **209**(1–2), 42–52 (2005).
7. C. K. Sun, C. C. Chen, S. W. Chu, T. H. Tsai, Y. C. Chen, and B. L. Lin, "Multiharmonic-generation biopsy of skin," *Opt. Lett.* **28**(24), 2488–2490 (2003).
8. C. K. Sun, S. W. Chu, S. Y. Chen, T. H. Tsai, T. M. Liu, C. Y. Lin, and H. J. Tsai, "Higher harmonic generation microscopy for developmental biology," *J. Struct. Biol.* **147**(1), 19–30 (2004).
9. S. P. Tai, T. H. Tsai, W. J. Lee, D. B. Shieh, Y. H. Liao, H. Y. Huang, K. Y. J. Zhang, H. L. Liu, and C. K. Sun, "Optical biopsy of fixed human skin with backward-collected optical harmonics signals," *Opt. Express* **13**(20), 8231–8242 (2005).
10. S. P. Tai, W. J. Lee, D. B. Shieh, P. C. Wu, H. Y. Huang, C. H. Yu, and C. K. Sun, "In vivo optical biopsy of hamster oral cavity with epi-third-harmonic-generation microscopy," *Opt. Express* **14**(13), 6178–6187 (2006).
11. S. Y. Chen, H. Y. Wu, and C. K. Sun, "In vivo harmonic generation biopsy of human skin," *J. Biomed. Opt.* **14**(6), 060505 (2009).
12. S. Y. Chen, S. U. Chen, H. Y. Wu, W. J. Lee, Y. H. Liao, and C. K. Sun, "In vivo virtual biopsy of human skin by using noninvasive higher harmonic generation microscopy," *IEEE J. Sel. Top. Quantum Electron.* **PP**(99), 1–15 (2009).
13. L. C. Kuypers, W. F. Decraemer, J. J. J. Dirckx, and J. P. Timmermans, "Thickness distribution of fresh eardrums of cat obtained with confocal microscopy," *J. Assoc. Res. Otolaryngol.* **6**(3), 223–233 (2005).
14. M. C. Chan, T. M. Liu, S. P. Tai, and C. K. Sun, "Compact fiber-delivered Cr:forsterite laser for nonlinear light microscopy," *J. Biomed. Opt.* **10**(5), 054006 (2005).
15. T. H. Tsai, S. P. Tai, W. J. Lee, H. Y. Huang, Y. H. Liao, and C. K. Sun, "Optical signal degradation study in fixed human skin using confocal microscopy and higher-harmonic optical microscopy," *Opt. Express* **14**(2), 749–758 (2006).
16. S. Y. Chen, H. C. Yu, I. J. Wang, and C. K. Sun, "Infrared-based third and second harmonic generation imaging of cornea," *J. Biomed. Opt.* **14**(4), 044012 (2009).
17. S. W. Chu, I. H. Chen, T. M. Liu, C. K. Sun, S. P. Lee, B. L. Lin, P. C. Cheng, M. X. Kuo, D. J. Lin, and H. L. Liu, "Nonlinear biophotonic crystal effects revealed with multimodal nonlinear microscopy," *J. Microsc.* **208**(3), 190–200 (2002).
18. G. Alzbutiene, A. Hermansson, P. Caye-Thomasen, and V. Kinduris, "Tympanic membrane changes in experimental acute otitis media and myringotomy," *Medicina (Kaunas)* **44**(4), 313–321 (2008).
19. K. Stenfeldt, C. Johansson, and S. Hellstrom, "The collagen structure of the tympanic membrane: collagen types I, II, and III in the healthy tympanic membrane, during healing of a perforation, and during infection," *Arch. Otolaryngol. Head Neck Surg.* **132**(3), 293–298 (2006).
20. K. N. O'Connor, M. Tam, N. H. Blevins, and S. Puria, "Tympanic membrane collagen fibers: a key to high-frequency sound conduction," *Laryngoscope* **118**(3), 483–490 (2008).
21. R. P. Jackson, C. Chlebicki, T. B. Krasieva, and S. Puria, "Multiphoton microscopy imaging of collagen fiber layers and orientation in the tympanic membrane," *Proc. SPIE* **6842**, 68421D (2008).